

A lowest order stabilization-free mixed Virtual Element Method

Andrea Borio, Carlo Lovadina, Francesca Marcon and Michele Visinoni

Abstract

We initiate the design and the analysis of stabilization-free Virtual Element Methods for the laplacian problem written in mixed form. A Virtual Element version of the lowest order Raviart-Thomas Finite Element is considered. To reduce the computational costs, a suitable projection on the gradients of harmonic polynomials is employed. A complete theoretical analysis of stability and convergence is developed in the case of quadrilateral meshes. Some numerical tests highlighting the actual behaviour of the scheme are also provided.

1 Introduction

In these years, the study of numerical methods for solving partial differential equations on polygonal/polytopal meshes has been experiencing a growing interest in the scientific community. In particular, one of the most recent developments in this field is represented by the Virtual Element Method (VEM). This technology was first introduced in the primal conforming Poisson problem in [2] as a generalization of H^1 -conforming Finite Element Method. Successively, the extension to the $H(\text{div})$ -conforming vector fields, generalizing Mixed Finite Elements [18], has been introduced in [22] and developed in [4, 3, 27]. Thanks to the great flexibility of the method, both primal and mixed formulation of VEM have been applied to a large range of applications, such as elastic and inelastic problems [7, 1, 25, 28], simulations in fractured media [8, 9, 10, 15] and in porous media mechanics [19, 16, 14], just to mention a few of them.

The key ideas of VEM may be summarised as follows.

- The local approximation spaces are defined as the solutions to suitable local partial differential problems. Therefore, VEM functions are not explicitly known, but only a limited information is available. However, the local approximation spaces contain polynomials up to a suitable degree.
- A computable projection onto a polynomial space is involved. Typically, the projection is valued onto the polynomials contained in the approximation spaces.
- The discrete bilinear forms are characterized by the sum of a singular part maintaining consistency on polynomials, and a stabilizing form enforcing coercivity.

However, in general the stabilising form mentioned above is designed without a clear physical meaning, but only requiring minimal assumptions to make the method stable. Though efficient recipes to tune the stabilisation term have been proposed (see for instance

[6, 26]), in certain complex situations it might be preferable to avoid dealing with the choice of such forms. As examples, we mention highly non-linear problems; problems where highly anisotropic meshes occurs; advection-diffusion problems. In addition, the stabilization term could be problematic in connection with the analysis of a-posteriori error estimates [23, 11] (however, the recent work [5] presents a first study which provides stabilization-free upper and lower a-posteriori bounds for triangular meshes with hanging nodes).

Virtual Element schemes for which no stabilisation form is required have been recently presented, in different 2D frameworks, in [12, 13, 30, 31]. These approaches share the idea to employ a projection onto a polynomial space of higher degree than the one usually taken in standard VEM. It is worth noticing that the polynomial degree depends on the number of edges of each polygon: as expected, it increases as the edge number gets larger. As a consequence, the quadrature computational cost significantly grows in presence of elements with many edges, without any improvement in the convergence rate.

This paper follows similar lines of the above-mentioned stabilisation-free attempts [12, 13, 30, 31], but for the Laplacian problem written in the usual $H(\text{div})-L^2$ mixed formulation. In particular, we consider a VEM version of the lowest order Raviart-Thomas Finite Element Method, see [4]. To reduce the computational cost connected to quadrature, a suitable projection operator onto the gradients of *harmonic* polynomials is selected, similarly to the scheme introduced for the primal formulation in [17]. The resulting scheme has the following features.

- It is a conforming mixed VEM method for which no stabilization term is needed.
- The method shows first order convergence rate for the natural norms and, in most cases, a behaviour comparable with the standard lowest order Raviart-Thomas VEM for which the stabilisation term is suitably tuned. However, for highly anisotropic meshes, our method seems to display a better performance.
- Despite a projection over higher-order polynomial spaces is employed, the use of *harmonic* polynomials greatly alleviate the additional computational costs.

These properties indicate that the present approach could be a valid alternative to the lowest order Raviart-Thomas Virtual Element Methods, especially in those complex situations where, for the latter scheme, a particular care in the treatment of the stabilising form is required.

From a theoretical point of view, the present paper can be considered as a first contribution, since we present a rigorous analysis only for the quadrilateral case (of course, the similar arguments could be applied also for triangular elements). However, the general theory for polygons with an arbitrary number of edges is not currently available and will be treated in a future work.

A brief outline of the paper is as follows. In Section 2 we define the model problem. Section 3 contains the statement of the discrete problems, introducing all the bilinear and linear forms involved. In section 4, we prove the well-posedness of the discrete problem in the quadrilateral case. For the same kind of meshes, we derive optimal error estimates in Section 5 and, finally, in Section 6 we present some numerical results that assess the convergence rate of the method; a comparison with the standard lowest order Raviart-Thomas VEM is also provided.

2 Model problem

Let $\Omega \subset \mathbb{R}^2$ be a computational domain. We are interested in studying the following mixed formulation of the Poisson problem:

$$\begin{cases} -\operatorname{div} \boldsymbol{\sigma} = f & \text{in } \Omega \\ \boldsymbol{\sigma} = \nabla u & \text{in } \Omega \\ u = 0 & \text{on } \partial\Omega \end{cases}, \quad (1)$$

where the forcing term $f \in L^2(\Omega)$. We consider homogeneous natural boundary conditions only for sake of simplicity: the extension to non-homogeneous or essential boundary conditions can be treated with the same techniques used for other more classical Galerkin methods, such as the FEM. Let $(\cdot, \cdot)_\Omega$ denote the L^2 scalar product and $a(\boldsymbol{\sigma}, \boldsymbol{\tau}) := (\boldsymbol{\sigma}, \boldsymbol{\tau})_\Omega$, then the mixed variational formulation of (1) is given by: find $(\boldsymbol{\sigma}, u) \in \Sigma \times U$, where $\Sigma := \mathbf{H}(\operatorname{div}, \Omega)$ and $U := L^2(\Omega)$ such that

$$\begin{cases} a(\boldsymbol{\sigma}, \boldsymbol{\tau}) + (\operatorname{div} \boldsymbol{\tau}, u)_\Omega = 0 & \forall \boldsymbol{\tau} \in \Sigma, \\ (\operatorname{div} \boldsymbol{\sigma}, v)_\Omega = -(f, v)_\Omega & \forall v \in U. \end{cases} \quad (2)$$

Well posedness of the above problem (2) is standard and the details can be found, for instance, in [18].

3 VEM discrete formulation

In order to state the discrete formulation of (2), let \mathcal{M}_h be a polygonal tessellation of Ω . For every element $E \in \mathcal{M}_h$, its area and diameter are denoted by $|E|$ and h_E , respectively. As usual, the maximum of the diameters h_E for $E \in \mathcal{M}_h$ is the mesh size, denoted by h , i.e. $h = \max_{E \in \mathcal{M}_h} h_E$. We assume that each $E \in \mathcal{M}_h$ is such that

A.1 E is star-shaped with respect to a ball of radius $\geq \gamma h_E$,

A.2 for any edge e of ∂E , $|e| \geq \gamma h_E$,

where γ is a positive constant.

To continue, for any given $E \in \mathcal{M}_h$ and non-negative integer k , $\mathbb{P}_k(E)$ denotes the space of polynomials of degree up to k defined on E . Moreover, we introduce $\mathbb{P}_k^H(E) \subseteq \mathbb{P}_k(E)$ as the space of *harmonic* polynomials of degree up to k defined on E ; the dimension of this latter space is $2k + 1$.

3.1 The local spaces

In this section we introduce the discrete local space and their interpolation properties. Given a generic quadrilateral $E \in \mathcal{M}_h$, we introduce the following local VEM space:

$$\Sigma_h(E) := \left\{ \boldsymbol{\tau}_h \in \mathbf{H}(\operatorname{div}, E) : \exists v \in \mathbf{H}^1(E) \text{ s.t. } \boldsymbol{\tau}_h = \nabla v, \right. \\ \left. \boldsymbol{\tau}_h \cdot \mathbf{n}_e \in \mathbb{P}_0(e) \quad \forall e \in \partial E, \quad \operatorname{div} \boldsymbol{\tau}_h \in \mathbb{P}_0(E) \right\}. \quad (3)$$

Accordingly, for the local space $\Sigma_h(E)$ the following degrees of freedom can be taken:

$$\boldsymbol{\tau}_h \rightarrow \frac{1}{|e|} \int_e \boldsymbol{\tau}_h \cdot \mathbf{n}_e \, \mathrm{d}e = \boldsymbol{\tau}_h \cdot \mathbf{n}_e, \quad \forall e \in \partial E. \quad (4)$$

The unisolvence of the above degrees of freedom is proved, e.g., as in [3], so that $\dim(\Sigma_h(E)) = 4$. We remark that, once $\boldsymbol{\tau}_h \cdot \mathbf{n}_e = c_e \in \mathbb{P}_0(E)$ is given for all $e \in \partial E$, the quantity $\operatorname{div} \boldsymbol{\tau}_h \in \mathbb{P}_0(E)$ is uniquely determined. Since $\operatorname{div} \boldsymbol{\tau}_h \in \mathbb{P}_0(E)$ then

$$\operatorname{div} \boldsymbol{\tau}_h = \frac{1}{|E|} \int_E \operatorname{div} \boldsymbol{\tau}_h \, dE = \frac{1}{|E|} \sum_{e \in \partial E} \int_e \boldsymbol{\tau}_h \cdot \mathbf{n}_e \, de = \frac{1}{|E|} \sum_{e \in \partial E} |e| c_e. \quad (5)$$

The local approximation space for U is simply defined as follows

$$U_h(E) := \{u_h \in L^2(E) : u_h \in \mathbb{P}_0(E)\}. \quad (6)$$

Accordingly, for the local space $U_h(E)$ the following degrees of freedom can be taken:

$$u_h \rightarrow \frac{1}{|E|} \int_E u_h \, dE. \quad (7)$$

It follows that $\dim(U_h(E)) = 1$.

3.2 Approximation in Σ_h and U_h

Let us consider the space $W(\Omega) = \mathbf{H}(\operatorname{div}, \Omega) \cap [L^r(\Omega)]^2$ ($r > 2$), equipped with the natural norm. We define an interpolation operator

$$\mathcal{I}_h : W(\Omega) \longrightarrow \Sigma_h \quad (8)$$

by requiring

$$\int_e (\boldsymbol{\varsigma} - \mathcal{I}_h \boldsymbol{\varsigma}) \cdot \mathbf{n}_e \, de = 0, \quad \forall \text{ edge } e \text{ of the elements in } \mathcal{M}_h. \quad (9)$$

Using the unisolvence of the degrees of freedom, e.g. see [3], it is not difficult to check that such a $\mathcal{I}_h \boldsymbol{\varsigma}$ exists and it is unique in Σ_h . This definition implies that for each $E \in \mathcal{M}_h$

$$\int_E \operatorname{div} (\boldsymbol{\varsigma} - \mathcal{I}_h \boldsymbol{\varsigma}) \, dE = 0. \quad (10)$$

Hence, since for each $E \in \mathcal{M}_h$ $\operatorname{div} \mathcal{I}_h \boldsymbol{\varsigma} \in \mathbb{P}_0(E)$, we obtain the *commuting diagram property*

$$\operatorname{div} \mathcal{I}_h \boldsymbol{\varsigma} = \Pi_{0,E}^0 \operatorname{div} \boldsymbol{\varsigma}, \quad (11)$$

where $\Pi_{0,E}^0 : L^2(E) \rightarrow \mathbb{P}_0(E)$ is the L^2 projection operator onto constants. We now remark that $(\mathcal{I}_h \boldsymbol{\varsigma})|_E = \nabla \varphi^*$, φ^* being the solution to the local (compatible) Neumann problem

$$\begin{cases} \Delta \varphi^* = \Pi_{0,E}^0 \operatorname{div} \boldsymbol{\varsigma} & \text{in } E \\ \nabla \varphi^* \cdot \mathbf{n}_e = \Pi_{0,e}^0 (\boldsymbol{\varsigma} \cdot \mathbf{n}_e) & \text{on every } e \text{ side of } \partial E, \end{cases} \quad (12)$$

where $\Pi_{0,e}^0$ denotes the L^2 projection operator onto the constant functions on e . Regularity results of elliptic equations and Sobolev embedding theorems shows that there exists $r^* > 2$ such that for $r \in (2, r^*]$ it holds

$$\|\mathcal{I}_h \boldsymbol{\varsigma}\|_{0,E} \leq C_{r^*} \|\boldsymbol{\varsigma}\|_{W(E)}. \quad (13)$$

Moreover assuming $\boldsymbol{\varsigma} \in [\mathbf{H}^1(\Omega)]^2$ and $\operatorname{div} \boldsymbol{\varsigma} \in \mathbf{H}^1(\Omega)$, the following approximation results hold: for each h , for each $E \in \mathcal{M}_h$

$$\|\operatorname{div}(\boldsymbol{\varsigma} - \mathcal{I}_h \boldsymbol{\varsigma})\|_{0,E} \leq C_d h_E^s |\operatorname{div} \boldsymbol{\varsigma}|_{s,E}, \quad s = 0, 1 \quad (14)$$

and

$$\|\boldsymbol{\varsigma} - \mathcal{I}_h \boldsymbol{\varsigma}\|_{0,E} \leq C_\varsigma h_E |\boldsymbol{\varsigma}|_{1,E}. \quad (15)$$

Above, C_{r^*} , C_d and C_ς are positive constants depending only on the constant γ of the mesh assumptions **A.1** and **A.2**.

Moreover, we recall that, given $w \in \mathbf{H}^1(\Omega) \cap \mathbf{L}^2(\Omega)$, for its \mathbf{L}^2 projection $\Pi_{0,E}^0 w \in U_h$ it holds for each h , for each $E \in \mathcal{M}_h$

$$\|w - \Pi_{0,E}^0 w\|_{0,E} \leq C h_E^s |w|_{s,E}, \quad s = 0, 1, \quad (16)$$

where $C > 0$ depends only on the constant γ of the mesh assumptions **A.1** and **A.2**.

3.3 The local forms

In this section we introduce the VEM counterparts of the local forms associated with the continuous problem.

The local mixed term Given $E \in \mathcal{M}_h$, we notice that the term

$$(\operatorname{div} \boldsymbol{\tau}_h, v_h)_E = \int_E v_h \operatorname{div} \boldsymbol{\tau}_h \, dE$$

is computable for every $\boldsymbol{\tau}_h \in \Sigma_h(E)$ and $v_h \in U_h(E)$ via degrees of freedom. For this reason, we do not need to introduce any approximation of the continuous terms $(\operatorname{div} \boldsymbol{\tau}, u)$ and $(\operatorname{div} \boldsymbol{\sigma}, v)$ in problem (2).

The local bilinear form $a^E(\cdot, \cdot)$ The local bilinear form

$$a^E(\boldsymbol{\sigma}_h, \boldsymbol{\tau}_h) = \int_E \boldsymbol{\sigma}_h \cdot \boldsymbol{\tau}_h \, dE$$

is not computable for a general pair $(\boldsymbol{\sigma}_h, \boldsymbol{\tau}_h) \in \Sigma_h(E) \times \Sigma_h(E)$. Here, instead of using the standard VEM procedure (cf. [4]), we introduce a local self-stabilized discrete bilinear form. Let

$$\hat{\Pi}_{k-1,E}^0 : [\mathbf{L}^2(E)]^2 \rightarrow \nabla \mathbb{P}_k^H(E) \quad (17)$$

be the $\mathbf{L}^2(E)$ -projection operator onto the space $\nabla \mathbb{P}_k^H(E)$, i.e. the space of gradients of *harmonic* polynomials of degree at most k , with $k \geq 1$. More precisely, $\hat{\Pi}_E^0$ is defined by the orthogonality condition: for each $\boldsymbol{\tau} \in [\mathbf{L}^2(E)]^2$, it holds

$$\left(\hat{\Pi}_{k-1,E}^0 \boldsymbol{\tau}, \nabla p \right)_E = (\boldsymbol{\tau}, \nabla p)_E, \quad \forall p \in \mathbb{P}_k^H(E). \quad (18)$$

In order to attain stability, the approximation of $a^E(\cdot, \cdot)$ depends on the number of edges of E , denoted by n_E . More precisely, $[\cdot]$ being the integer part, we select

$$k = \left\lceil \frac{n_E + 1}{2} \right\rceil \quad (19)$$

(i.e. k is the smallest integer such that $2k \geq n_E$). We then use the corresponding projection $\hat{\Pi}_E^0$, see (17) and (18), to define

$$a_h^E(\boldsymbol{\sigma}_h, \boldsymbol{\tau}_h) = \left(\hat{\Pi}_{k-1,E}^0 \boldsymbol{\sigma}_h, \hat{\Pi}_{k-1,E}^0 \boldsymbol{\tau}_h \right)_E \quad \forall \boldsymbol{\sigma}_h, \boldsymbol{\tau}_h \in \Sigma_h(E). \quad (20)$$

Remark 1. We remark that, although a rigorous analysis is still missing for general polygons, the numerical tests (see Section 6.1) seem to suggest that the choice (19) always leads to a stable scheme.

Remark 2. Given $\boldsymbol{\tau} \in \Sigma_h(E)$, to compute $\hat{\Pi}_{k-1,E}^0 \boldsymbol{\tau}_h$ one has solve, from (18) and integrating by parts:

$$\left(\hat{\Pi}_{k-1,E}^0 \boldsymbol{\tau}_h, \nabla p \right)_E = -(\operatorname{div} \boldsymbol{\tau}_h, p)_E + \int_{\partial E} (\boldsymbol{\tau}_h \cdot \mathbf{n}) p \, de, \quad \forall p \in \mathbb{P}_k^H(E), \quad (21)$$

which is clearly computable, as $\operatorname{div} \boldsymbol{\tau}_h$ is computable and constant. Moreover, integrating by parts also the left-hand side and taking into account that the involved polynomials are harmonic, one realizes that the integral over E can be computed as an integral over ∂E ; therefore, only 1D quadrature rules are required to compute the left-hand side of (21). Furthermore, since $\operatorname{div} \boldsymbol{\tau}_h$ is constant, the first term in the right-hand side requires only to evaluate the integral of a harmonic polynomial of degree at most k . Hence, the computation of $\hat{\Pi}_{k-1,E}^0 \boldsymbol{\tau}_h$ is not as cumbersome as it may appear at a first sight.

The local right-hand side term We split the right-hand side term on each quadrilateral and we have

$$(f, v_h)_E = \int_E f v_h \, dE.$$

Since $v_h \in U_h(E) = \mathbb{P}_0(E)$, we have that

$$(f, v_h) = \sum_{E \in \mathcal{M}_h} v_h \int_E f \, dE,$$

which is computable via quadrature rules for polygonal domains, see for instance [32].

3.4 The discrete scheme

Starting from the local spaces and local terms introduced in the previous sections, we can set the global self-stabilized problem. More specifically, we introduce these two global approximation spaces, by gluing the local approximation spaces, see (3) and (6):

$$\Sigma_h = \{ \boldsymbol{\tau}_h \in \mathbf{H}(\operatorname{div}, \Omega) : \boldsymbol{\tau}_{h|_E} \in \Sigma_h(E), \quad \forall E \in \mathcal{M}_h \} \quad (22)$$

and

$$U_h = \{ u_h \in U : u_{h|_E} \in U_h(E), \quad \forall E \in \mathcal{M}_h \}. \quad (23)$$

Now, given a local approximation of $a^E(\cdot, \cdot)$, see (20), $\forall \boldsymbol{\sigma}_h, \boldsymbol{\tau}_h \in \Sigma_h$ we set

$$a_h(\boldsymbol{\sigma}_h, \boldsymbol{\tau}_h) := \sum_{E \in \mathcal{M}_h} a_h^E(\boldsymbol{\sigma}_h, \boldsymbol{\tau}_h). \quad (24)$$

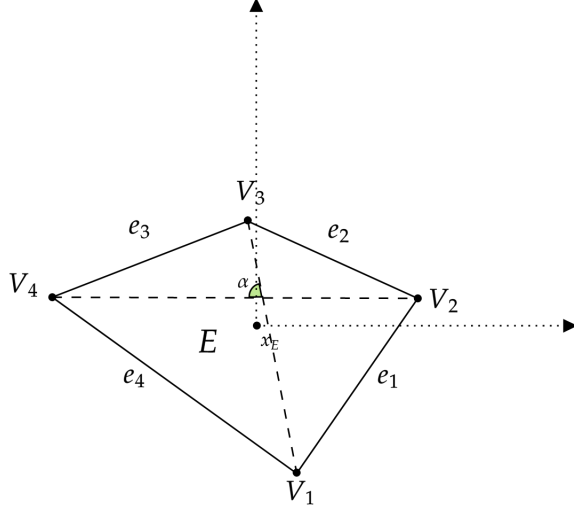


Figure 1: A general quadrilateral $E \in \mathcal{M}_h$

We can state the discrete problem as: find $(\boldsymbol{\sigma}_h, u_h) \in \Sigma_h \times U_h$ such that

$$\begin{cases} a_h(\boldsymbol{\sigma}_h, \boldsymbol{\tau}_h) + (\operatorname{div} \boldsymbol{\tau}_h, u_h)_\Omega = 0 & \forall \boldsymbol{\tau}_h \in \Sigma_h \\ (\operatorname{div} \boldsymbol{\sigma}_h, v_h)_\Omega = (f, v_h)_\Omega & \forall v_h \in U_h \end{cases} \quad (25)$$

In the next section we focus on the well-posedness of this discrete scheme, in the case of quadrilateral meshes, which requires in particular the coercivity-on-the-kernel condition for the bilinear form $a_h(\cdot, \cdot)$ (also called *ellipticity-on-the-kernel condition*).

4 Well-posedness in the quadrilateral case

From now on we focus on the case where the mesh \mathcal{M}_h is made up by quadrilaterals. This implies that we choose $k = 2$, so that we use the local projection $\hat{\Pi}_{1,E}^0$, see (19). Hence, we project onto the gradients of quadratic harmonic polynomials, a space of dimension 4. For each quadrilateral $E \in \mathcal{M}_h$, V_i (for $i = 1, \dots, 4$) denote its vertices counterclockwise ordered and e_i the edge connecting V_i to V_{i+1} , where $V_5 = V_1$ (see Figure. 1). Let \mathbf{n}_i , be the unit normal vector of the edges e_i for $i = 1, \dots, 4$. This section is devoted to prove the well-posedness of the discrete problem stated by (25).

We introduce the following two useful spaces $\operatorname{RT}_0(E)$ and $\operatorname{H}(E)$, and we prove some properties of their functions.

Definition 1 (Raviart-Thomas space $\operatorname{RT}_0(E)$). *It is the space of the polynomial functions defined as follows:*

$$\operatorname{RT}_0(E) := \left\{ \mathbf{r} \in [\mathbb{L}^2(E)]^2 : \mathbf{r} = \begin{pmatrix} c_1 \\ c_2 \end{pmatrix} + c_3 \begin{pmatrix} x \\ y \end{pmatrix}, \quad s.t. \quad c_1, c_2, c_3 \in \mathbb{R} \right\}, \quad (26)$$

whose dimension is equal to 3.

Definition 2 (Hourglass space $H(E)$). Let $\boldsymbol{\xi} \in \Sigma_h(E)$ be the function such that

$$\boldsymbol{\xi} \cdot \mathbf{n}_j = \frac{(-1)^j}{|e_j|} \quad \forall j = 1, \dots, 4, \quad (27)$$

then we introduce the following one dimensional virtual space

$$H(E) := \text{span}(\boldsymbol{\xi}). \quad (28)$$

Using the divergence theorem, it is straightforward to see that a function $\tilde{\boldsymbol{\tau}}_h \in H(E)$ satisfies $\text{div } \tilde{\boldsymbol{\tau}}_h = 0$.

Remark 3. We notice that the two spaces above are two subspaces of $\Sigma_h(E)$.

Proposition 1. Let $\text{RT}_0(E)$ be the space defined in (26) and let $H(E)$ be the space defined in (28), then

$$\Sigma_h(E) = \text{RT}_0(E) \oplus H(E). \quad (29)$$

Moreover, let us define the local divergence-free subspace:

$$\Sigma_h^0(E) = \{\boldsymbol{\tau}_h \in \Sigma_h(E) : \text{div } \boldsymbol{\tau}_h = 0\}. \quad (30)$$

Then it holds

$$\Sigma_h^0(E) = (\mathbb{P}_0(E))^2 \oplus H(E) \quad (31)$$

and the decomposition is L^2 -orthogonal.

Proof. Notice that, according to the dimension of $\text{RT}_0(E)$ and $H(E)$, to get (29) we only have to prove that $\text{RT}_0(E) \cap H(E) = \{\mathbf{0}\}$, that is $\boldsymbol{\xi} \notin \text{RT}_0(E)$. By contradiction, we suppose that $\boldsymbol{\xi} \in \text{RT}_0(E)$. Notice that by definition of $\boldsymbol{\xi}$, $\text{div } \boldsymbol{\xi} = 0$, hence $\boldsymbol{\xi} \in (\mathbb{P}_0(E))^2$. Take now $\mathbf{a} = \nabla(\mathbf{a} \cdot \mathbf{x})$, where $\mathbf{a} \in (\mathbb{P}_0(E))^2$. We have, using integration by parts and (27):

$$(\boldsymbol{\xi}, \mathbf{a})_E = (\boldsymbol{\xi}, \nabla(\mathbf{a} \cdot \mathbf{x}))_E = \int_{\partial E} (\boldsymbol{\xi} \cdot \mathbf{n}_E)(\mathbf{a} \cdot \mathbf{x}) = \sum_{i=1}^4 \int_{e_i} \frac{(-1)^i}{|e_i|} (\mathbf{a} \cdot \mathbf{x}), \quad (32)$$

for every $\mathbf{a} \in (\mathbb{P}_0(E))^2$. An application of the trapezoidal rule gives

$$(\boldsymbol{\xi}, \mathbf{a})_E = \mathbf{a} \cdot \left(\frac{1}{2} \sum_{j=1}^4 (-1)^j (V_j + V_{j+1}) \right) = 0 \quad \forall \mathbf{a} \in (\mathbb{P}_0(E))^2. \quad (33)$$

Recalling that $\boldsymbol{\xi}$ is constant, from (33) we infer $\boldsymbol{\xi} = \mathbf{0}$, a contradiction since $\boldsymbol{\xi} \neq 0$. Furthermore, decomposition (31) follows from a dimensional count, while the L^2 -orthogonality is simply (33). \square

Lemma 1. Let $E \in \mathcal{M}_h$ and let $\boldsymbol{\xi}$ be the hourglass function defined on E by (27). Then $\exists C_\boldsymbol{\xi} > 0$ independent of h_E such that

$$\|\boldsymbol{\xi}\|_0 \leq C_\boldsymbol{\xi}. \quad (34)$$

Proof. Since $\boldsymbol{\xi} \in \Sigma_h(E)$, by (3) $\exists v \in H^1(E)$ such that $\boldsymbol{\xi} = \nabla v$. It is clear that v is defined up to a constant, so we choose v such that $\int_E v = 0$. This implies that $\exists C > 0$ independent of h_E such that

$$\|v\|_0 \leq Ch_E \|\nabla v\|_0 = Ch_E \|\boldsymbol{\xi}\|_0, \quad (35)$$

by Poincaré's inequality. Moreover, since $\operatorname{div} \boldsymbol{\xi} = 0$, it holds $\Delta v = 0$. Then, by Green's theorem and a Cauchy-Schwarz inequality we have

$$\|\boldsymbol{\xi}\|_0^2 = (\boldsymbol{\xi}, \nabla v)_E = (\boldsymbol{\xi} \cdot \mathbf{n}, v)_{\partial E} \leq \|\boldsymbol{\xi} \cdot \mathbf{n}\|_{0, \partial E} \|v\|_{0, \partial E}. \quad (36)$$

We can apply a standard trace inequality to the last norm and obtain, by exploiting also (35),

$$\|v\|_{0, \partial E} \leq h_E^{\frac{1}{2}} \left(h_E^{-2} \|v\|_0^2 + \|\nabla v\|_0^2 \right)^{\frac{1}{2}} \leq Ch_E^{\frac{1}{2}} \|\boldsymbol{\xi}\|_0. \quad (37)$$

On the other hand, an explicit computation exploiting the definition of $\boldsymbol{\xi}$ given by (27) yields

$$\|\boldsymbol{\xi} \cdot \mathbf{n}\|_{0, \partial E}^2 = \sum_{j=1}^4 \int_{e_j} \left[\frac{(-1)^j}{|e_j|} \right]^2 = \sum_{j=1}^4 |e_j|^{-1} \leq 4\gamma^{-1} h_E^{-1}, \quad (38)$$

where the last inequality is obtained by exploiting the mesh assumption **A.2**. Using (37) and (38) into (36), we get

$$\|\boldsymbol{\xi}\|_0^2 \leq \|\boldsymbol{\xi} \cdot \mathbf{n}\|_{0, \partial E} \|v\|_{0, \partial E} \leq 2\gamma^{-\frac{1}{2}} h_E^{-\frac{1}{2}} \cdot Ch_E^{\frac{1}{2}} \|\boldsymbol{\xi}\|_0 \leq C \|\boldsymbol{\xi}\|_0,$$

which yields the thesis. \square

Lemma 2. *Under the mesh assumptions **A.1** and **A.2**, for every $E \in \mathcal{M}_h$, there exists a positive constant C_* , independent of h_E , such that*

$$\left\| \hat{\Pi}_{1,E}^0 \tilde{\boldsymbol{\tau}}_h \right\|_0 \geq C_* \|\tilde{\boldsymbol{\tau}}_h\|_0 \quad \forall \tilde{\boldsymbol{\tau}}_h \in \mathbf{H}(E). \quad (39)$$

Proof. Since $\mathbf{H}(E) = \operatorname{span}(\boldsymbol{\xi})$, it is sufficient to prove (39) for $\tilde{\boldsymbol{\tau}}_h = \boldsymbol{\xi}$. Using the definition of the norm of the operator $\hat{\Pi}_E^0$ and (18), we have

$$\left\| \hat{\Pi}_{1,E}^0 \boldsymbol{\xi} \right\|_0 = \sup_{\mathbf{q} \in \nabla \mathbb{P}_2^H(E)} \frac{\left(\hat{\Pi}_{1,E}^0 \boldsymbol{\xi}, \mathbf{q} \right)}{\|\mathbf{q}\|_0} = \sup_{\mathbf{q} \in \nabla \mathbb{P}_2^H(E)} \frac{(\boldsymbol{\xi}, \mathbf{q})}{\|\mathbf{q}\|_0}. \quad (40)$$

By Varignon's theorem [24], for each element $E \in \mathcal{M}_h$, the quadrilateral K_E whose vertices are the edge midpoints M_j ($j = 1, \dots, 4$) of E , is a parallelogram. With the usual abuse of notation that $V_5 = V_1$ we have

$$M_j = \frac{V_j + V_{j+1}}{2},$$

and the area of K_E satisfies $|K_E| = \frac{|E|}{2}$. Under the mesh assumptions **A.1** and **A.2**, it is not hard to show that the parallelogram is not degenerate, i.e. assumptions **A.1** and **A.2** hold for K_E as well. We now construct $p^* \in \mathbb{P}_2^H(E)$ such that

$$p^*(M_j) = (-1)^j, \quad \text{for each } j = 1, \dots, 4. \quad (41)$$

To this aim, it is useful to resort to complex numbers $z = x + iy$. Hence, up to a translation, we can identify M_1 as $0 \in \mathbb{C}$; accordingly, we also set $M_2 = z_1$, $M_4 = z_2$ and $M_3 = z_1 + z_2$. A direct computation shows that the complex-valued polynomial

$$q(z) = -1 + 2 \frac{z_1 + z_2}{z_1 z_2} z - \frac{2}{z_1 z_2} z^2$$

satisfies conditions (41) (with the above-mentioned identifications of M_j). We now set $p^*(x, y) = \operatorname{Re}(q(z))$, where $z = x + iy$ and $\operatorname{Re}(\cdot)$ denotes the real part. The real-valued polynomial p^* is harmonic and satisfies conditions (41) as well. Let $\mathbf{p}^* := \nabla p^*$; from (40) we get

$$\left\| \hat{\Pi}_{1,E}^0 \boldsymbol{\xi} \right\|_0 \geq \frac{(\boldsymbol{\xi}, \mathbf{p}^*)}{\|\mathbf{p}^*\|_0}. \quad (42)$$

By an explicit computation using Cavalieri-Simpson's quadrature rule and (41), we have that

$$\begin{aligned} (\boldsymbol{\xi}, \mathbf{p}^*) &= \int_E \boldsymbol{\xi} \cdot \nabla p^* \, dE = \int_{\partial E} (\boldsymbol{\xi} \cdot \mathbf{n}) p^* \, de = \sum_{j=1}^4 \frac{(-1)^j}{|e_j|} \int_{e_j} p^* \, de \\ &= \sum_{j=1}^4 \frac{(-1)^j}{6} (p^*(V_j) + 4p^*(M_j) + p^*(V_{j+1})) \\ &= \sum_{j=1}^4 \frac{2}{3} (-1)^j p^*(M_j) = \frac{8}{3}. \end{aligned} \quad (43)$$

We now notice that, due to assumptions **A.1** and **A.2**, there exists $C_{\mathbf{p}^*} > 0$, independent of h_E , such that $\|\mathbf{p}^*\|_0 = \|\nabla p^*\|_0 \leq C_{\mathbf{p}^*}$. Therefore, using Lemma 1 we have

$$\left\| \hat{\Pi}_{1,E}^0 \boldsymbol{\xi} \right\|_0 \geq \frac{8}{3 \|\mathbf{p}^*\|_0} = \frac{8 \|\boldsymbol{\xi}\|_0}{3 \|\boldsymbol{\xi}\|_0 \|\mathbf{p}^*\|_0} \geq \frac{8}{3 C_{\boldsymbol{\xi}} C_{\mathbf{p}^*}} \|\boldsymbol{\xi}\|_0. \quad (44)$$

Then, (39) holds with $C_* = \frac{8}{3 C_{\boldsymbol{\xi}} C_{\mathbf{p}^*}}$. \square

4.1 Continuity and coercivity of the local bilinear form $a_h^E(\cdot, \cdot)$

In this section, applying the above preliminary results, in particular Lemma 2, we prove the continuity and coercivity (on the divergence operator kernel) of the local bilinear form $a_h^E(\cdot, \cdot)$ in the L^2 -norm.

Theorem 1. *Under the mesh assumptions **A.1** and **A.2**, for every $E \in \mathcal{M}_h$, the discrete bilinear form $a_h^E(\cdot, \cdot)$, defined in (20), is L^2 continuous and coercive-on-the kernel, namely there exist two positive constants α_* and α^* , independent of h_E , such that*

$$a_h^E(\boldsymbol{\tau}_h, \boldsymbol{\sigma}_h) \leq \alpha^* \|\boldsymbol{\tau}_h\|_0 \|\boldsymbol{\sigma}_h\|_0, \quad \forall \boldsymbol{\tau}_h, \boldsymbol{\sigma}_h \in \Sigma_h(E) \quad (45)$$

and

$$a_h^E(\boldsymbol{\tau}_h, \boldsymbol{\tau}_h) \geq \alpha_* \|\boldsymbol{\tau}_h\|_0^2, \quad \forall \boldsymbol{\tau}_h \in \Sigma_h^0(E), \quad (46)$$

where Σ_h^0 is the divergence-free subspace defined in (30).

Proof. Fixed an element $E \in \mathcal{M}_h$, we first check the continuity. For every $\boldsymbol{\tau}_h, \boldsymbol{\sigma}_h \in \Sigma_h(E)$, applying the definition of $\hat{\Pi}_E^0$, its continuity and the Cauchy-Schwarz inequality, we obviously obtain

$$a_h^E(\boldsymbol{\tau}_h, \boldsymbol{\sigma}_h) = (\hat{\Pi}_{1,E}^0 \boldsymbol{\tau}_h, \hat{\Pi}_{1,E}^0 \boldsymbol{\sigma}_h) \leq \|\boldsymbol{\tau}_h\|_0 \|\boldsymbol{\sigma}_h\|_0. \quad (47)$$

Then (45) holds with $\alpha^* = 1$.

Now, we prove the Σ_h^0 -coercivity of the bilinear form $a_h^E(\cdot, \cdot)$. From Proposition 1, we get that every $\boldsymbol{\tau}_h \in \Sigma_h^0$ can be written by means of the orthogonal decomposition

$$\boldsymbol{\tau}_h = \boldsymbol{\tau}_0 + \tilde{\boldsymbol{\tau}}_h,$$

where $\boldsymbol{\tau}_0 \in (\mathbb{P}_0(E))^2$ and $\tilde{\boldsymbol{\tau}}_h \in \mathbf{H}(E)$. Moreover, one has

$$\|\boldsymbol{\tau}_h\|_0^2 = \|\boldsymbol{\tau}_0\|_0^2 + \|\tilde{\boldsymbol{\tau}}_h\|_0^2.$$

Using Lemma 2, the definition of the projection operator (18) and noticing that $\hat{\Pi}_{1,E}^0 \boldsymbol{\tau}_0 = \boldsymbol{\tau}_0$, we have

$$\begin{aligned} a_h^E(\boldsymbol{\tau}_h, \boldsymbol{\tau}_h) &= \left(\hat{\Pi}_{1,E}^0 \boldsymbol{\tau}_h, \hat{\Pi}_{1,E}^0 \boldsymbol{\tau}_h \right) = \left(\hat{\Pi}_{1,E}^0 \boldsymbol{\tau}_0 + \hat{\Pi}_{1,E}^0 \tilde{\boldsymbol{\tau}}_h, \hat{\Pi}_{1,E}^0 \boldsymbol{\tau}_0 + \hat{\Pi}_{1,E}^0 \tilde{\boldsymbol{\tau}}_h \right) \\ &= (\boldsymbol{\tau}_0, \boldsymbol{\tau}_0) + 2(\boldsymbol{\tau}_0, \tilde{\boldsymbol{\tau}}_h) + \left(\hat{\Pi}_{1,E}^0 \tilde{\boldsymbol{\tau}}_h, \hat{\Pi}_{1,E}^0 \tilde{\boldsymbol{\tau}}_h \right) \\ &= (\boldsymbol{\tau}_0, \boldsymbol{\tau}_0) + \left(\hat{\Pi}_{1,E}^0 \tilde{\boldsymbol{\tau}}_h, \hat{\Pi}_{1,E}^0 \tilde{\boldsymbol{\tau}}_h \right) \\ &\geq (\boldsymbol{\tau}_0, \boldsymbol{\tau}_0) + C_* (\tilde{\boldsymbol{\tau}}_h, \tilde{\boldsymbol{\tau}}_h) \\ &\geq \min \{1, C_*\} [\|\boldsymbol{\tau}_0\|_0^2 + \|\tilde{\boldsymbol{\tau}}_h\|_0^2] \\ &= C_* \|\boldsymbol{\tau}_h\|_0^2, \end{aligned} \quad (48)$$

which yields the thesis, with $\alpha_* = C_*$. \square

4.2 Ellipticity-on-the-kernel condition and inf-sup condition

In this section, we consider the two conditions, i.e. the coercivity of the bilinear form $a_h^E(\cdot, \cdot)$ on the kernel of the mixed term and the LBB inf-sup condition, that imply the well-posedness of the discrete problem (25).

Let us introduce the discrete kernel space given by

$$K_h := \{ \boldsymbol{\tau}_h \in \Sigma_h : (\operatorname{div} \boldsymbol{\tau}_h, v_h) = 0 \forall v_h \in U_h \}. \quad (49)$$

Notice that $\forall \boldsymbol{\tau}_h \in K_h$ we have that $\operatorname{div} \boldsymbol{\tau}_h = 0$, so that $\boldsymbol{\tau}_h|_E \in \Sigma_h^0$ and $\|\boldsymbol{\tau}_h\|_\Sigma = \|\boldsymbol{\tau}_h\|_0$. Hence, applying the local coercivity property (46) stated in Theorem 1 and the definition of the bilinear form $a_h(\cdot, \cdot)$ (24), we obtain that $\exists C_* > 0$, independent of h , such that

$$a_h(\boldsymbol{\tau}_h, \boldsymbol{\tau}_h) \geq C_* \|\boldsymbol{\tau}_h\|_\Sigma^2, \quad \forall \boldsymbol{\tau}_h \in K_h. \quad (50)$$

Furthermore, the inf-sup condition, i.e. $\exists \beta > 0$, independent of h , such that

$$\inf_{v \in U_h} \sup_{\boldsymbol{\tau}_h \in \Sigma_h} \frac{(\operatorname{div} \boldsymbol{\tau}_h, v)_\Omega}{\|v\|_0 \|\boldsymbol{\tau}_h\|_\Sigma} \geq \beta. \quad (51)$$

is a consequence of the so-called *Fortin's trick*, cf. [18], when the interpolation operator \mathcal{I}_h of Section 3.2 is considered (see in particular (10), (13) and (14) with $s = 0$).

5 Error estimates in the quadrilateral case

We prove optimal a priori error estimates for the method presented in this work, when the mesh is made up by quadrilaterals. We remark that the proof follows the usual guidelines for the VEM mixed schemes; however, we provide all the details, for the sake of completeness.

Theorem 2. *Let $(\boldsymbol{\sigma}, u) \in [\mathbf{H}^1(\Omega)]^2 \times \mathbf{H}_0^1(\Omega)$ and $f \in \mathbf{H}^1(\Omega)$ be respectively solution and forcing term of (2). Then $\exists C > 0$, independent of h , such that the unique solution $(\boldsymbol{\sigma}_h, u_h) \in \Sigma_h \times U_h$ of (25) satisfies the following error estimates:*

$$\|\boldsymbol{\sigma} - \boldsymbol{\sigma}_h\|_0 \leq Ch |\boldsymbol{\sigma}|_1, \quad (52)$$

$$\|\operatorname{div}(\boldsymbol{\sigma} - \boldsymbol{\sigma}_h)\|_0 \leq Ch |f|_1, \quad (53)$$

$$\|u - u_h\|_0 \leq Ch (|u|_1 + |\boldsymbol{\sigma}|_1). \quad (54)$$

Proof. In order to prove (52), let $\boldsymbol{\sigma}_I := \mathcal{I}_h \boldsymbol{\sigma} \in \Sigma_h$ be the interpolant of $\boldsymbol{\sigma}$ defined in Section 3.2. Then, applying the triangle inequality we obtain

$$\|\boldsymbol{\sigma} - \boldsymbol{\sigma}_h\|_0 \leq \|\boldsymbol{\sigma} - \boldsymbol{\sigma}_I\|_0 + \|\boldsymbol{\sigma}_I - \boldsymbol{\sigma}_h\|_0. \quad (55)$$

Let us focus on the term $\|\boldsymbol{\sigma}_I - \boldsymbol{\sigma}_h\|_0$. Notice that, applying the second equation of discrete problem (25) and the property of the interpolant (11), we have for each $E \in \mathcal{M}_h$

$$\operatorname{div} \boldsymbol{\sigma}_h = -\Pi_{0,E}^0 f = \Pi_{0,E}^0 \operatorname{div} \boldsymbol{\sigma} = \operatorname{div} \boldsymbol{\sigma}_I \implies \operatorname{div}(\boldsymbol{\sigma}_I - \boldsymbol{\sigma}_h) = 0, \quad (56)$$

hence $(\boldsymbol{\sigma}_I - \boldsymbol{\sigma}_h)|_E \in \Sigma_h^0$ for each $E \in \mathcal{M}_h$ (therefore $(\boldsymbol{\sigma}_I - \boldsymbol{\sigma}_h) \in K_h$). Notice that applying this relation to the first equation of the discrete problem (25) and to the first equation of the continuous problem (2) we obtain that $a_h(\boldsymbol{\sigma}_h, \boldsymbol{\sigma}_I - \boldsymbol{\sigma}_h) = 0$ and $a(\boldsymbol{\sigma}, \boldsymbol{\sigma}_I - \boldsymbol{\sigma}_h) = 0$. Then, since $\boldsymbol{\sigma}_I - \boldsymbol{\sigma}_h \in K_h$ we can apply Theorem (1), in particular (46), and obtain the estimate

$$\begin{aligned} \alpha_* \|\boldsymbol{\sigma}_I - \boldsymbol{\sigma}_h\|_0^2 &\leq a_h(\boldsymbol{\sigma}_I - \boldsymbol{\sigma}_h, \boldsymbol{\sigma}_I - \boldsymbol{\sigma}_h) \\ &= a_h(\boldsymbol{\sigma}_I, \boldsymbol{\sigma}_I - \boldsymbol{\sigma}_h) \\ &= \sum_{E \in \mathcal{M}_h} \left(a_h^E(\boldsymbol{\sigma}_I - \hat{\Pi}_{1,E}^0 \boldsymbol{\sigma}, \boldsymbol{\sigma}_I - \boldsymbol{\sigma}_h) + a_h^E(\hat{\Pi}_{1,E}^0 \boldsymbol{\sigma}, \boldsymbol{\sigma}_I - \boldsymbol{\sigma}_h) \right) \\ &= \sum_{E \in \mathcal{M}_h} \left(a_h^E(\boldsymbol{\sigma}_I - \hat{\Pi}_{1,E}^0 \boldsymbol{\sigma}, \boldsymbol{\sigma}_I - \boldsymbol{\sigma}_h) + a^E(\hat{\Pi}_{1,E}^0 \boldsymbol{\sigma}, \boldsymbol{\sigma}_I - \boldsymbol{\sigma}_h) \right) \\ &= \sum_{E \in \mathcal{M}_h} \left(a_h^E(\boldsymbol{\sigma}_I - \hat{\Pi}_{1,E}^0 \boldsymbol{\sigma}, \boldsymbol{\sigma}_I - \boldsymbol{\sigma}_h) + a^E(\hat{\Pi}_{1,E}^0 \boldsymbol{\sigma} - \boldsymbol{\sigma}, \boldsymbol{\sigma}_I - \boldsymbol{\sigma}_h) \right), \end{aligned} \quad (57)$$

where the projector $\hat{\Pi}_{1,E}^0$ is defined by the orthogonality condition (18) and satisfies, for each $E \in \mathcal{M}_h$, $a_h^E(\hat{\Pi}_{1,E}^0 \boldsymbol{\sigma}, \boldsymbol{\tau}_h) = a^E(\hat{\Pi}_{1,E}^0 \boldsymbol{\sigma}, \boldsymbol{\tau}_h) \forall \boldsymbol{\tau}_h \in \Sigma_h$. We now notice that, since $\boldsymbol{\sigma} = \nabla u$ and $\hat{\Pi}_{1,E}^0$ projects onto the space $\nabla \mathbb{P}_2^H(E)$, it holds

$$\left\| \boldsymbol{\sigma} - \hat{\Pi}_{1,E}^0 \boldsymbol{\sigma} \right\|_{0,E} = \left\| \nabla u - \hat{\Pi}_{1,E}^0(\nabla u) \right\|_{0,E} = \inf_{p \in \mathbb{P}_2^H(E)} |u - p|_{1,E} \leq Ch_E |\boldsymbol{\sigma}|_{1,E}, \quad (58)$$

where the last estimate follows from the standard approximation theory, see [20, 29, 21]. Then, by the continuity of $a_h^E(\cdot, \cdot)$ and $a^E(\cdot, \cdot)$, applying estimates (15) and (58), we obtain

$$\begin{aligned} \|\sigma_I - \sigma_h\|_0 &\leq C \sum_{E \in \mathcal{M}_h} \left(\|\sigma_I - \hat{\Pi}_{1,E}^0 \sigma\|_{0,E} + \|\sigma - \hat{\Pi}_{1,E}^0 \sigma\|_{0,E} \right) \\ &\leq C \left(\|\sigma - \sigma_I\|_0 + \sum_{E \in \mathcal{M}_h} \|\sigma - \hat{\Pi}_{1,E}^0 \sigma\|_{0,E} \right) \\ &\leq Ch |\sigma|_1 . \end{aligned} \quad (59)$$

Applying this relation and the interpolation estimate (15) to (55), estimate (52) is proved. Moreover, to prove (53) we apply (56), the interpolation estimate (14) and the equation $\operatorname{div} \sigma = -f$, to obtain

$$\|\operatorname{div} \sigma - \operatorname{div} \sigma_h\|_0 \leq \|\operatorname{div} \sigma - \operatorname{div} \sigma_I\|_0 \leq Ch |f|_1 . \quad (60)$$

Finally, we have to prove (54). Let $u_I := \Pi_{0,h}^0 u \in U_h$. Notice that by its definition u_I satisfies $(u - u_I, \operatorname{div} \tau_h)_\Omega = 0$ for each $\tau_h \in \Sigma_h$. By triangle inequality we have

$$\|u - u_h\|_0 \leq \|u - u_I\|_0 + \|u_I - u_h\|_0 . \quad (61)$$

First, let us consider the term $\|u_I - u_h\|_0$. Since $u_I - u_h \in U_h$, according to the inf-sup condition (51), there exists $\tau_h^* \in \Sigma_h$ be such that $\operatorname{div} \tau_h^* = u_I - u_h$ and

$$\|\tau_h^*\|_0 \leq \frac{1}{\beta} \|u_I - u_h\|_0 . \quad (62)$$

Then, applying the continuous problem (2), the discrete one (25) and adding and subtracting $\hat{\Pi}_E^0 \sigma$, we obtain

$$\begin{aligned} \|u_I - u_h\|_0^2 &= (u_I - u_h, \operatorname{div} \tau_h^*)_\Omega \\ &= (u - u_h, \operatorname{div} \tau_h^*)_\Omega \\ &= a(\sigma, \tau_h^*) - a_h(\sigma_h, \tau_h^*) \\ &= \sum_{E \in \mathcal{M}_h} a^E(\sigma - \hat{\Pi}_{1,E}^0 \sigma, \tau_h^*) + a_h^E(\hat{\Pi}_{1,E}^0 \sigma - \sigma_h, \tau_h^*) \\ &\leq C \sum_{E \in \mathcal{M}_h} \left(\|\sigma - \hat{\Pi}_{1,E}^0 \sigma\|_{0,E} + \|\sigma - \sigma_h\|_{0,E} \right) \|u_I - u_h\|_0 \end{aligned} \quad (63)$$

where in the last step we exploit the continuity of the bilinear forms together with (62). Finally, applying (63) to (61), the interpolation estimate (16) and the error estimate of σ (52) already proved, we obtain

$$\begin{aligned} \|u - u_h\|_0 &\leq \|u - u_I\|_0 + C \left(\sum_{E \in \mathcal{M}_h} \|\sigma - \hat{\Pi}_{1,E}^0 \sigma\|_{0,E} + \|\sigma - \sigma_h\|_0 \right) \\ &\leq Ch (|u|_1 + |\sigma|_1) . \end{aligned} \quad (64)$$

□

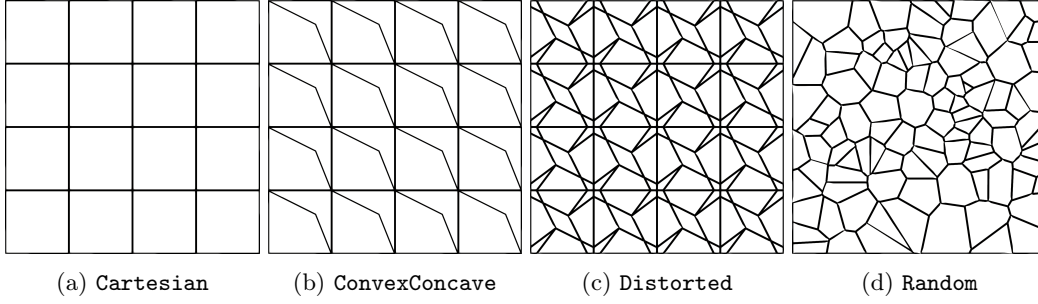


Figure 2: Meshes.

6 Numerical Tests

6.1 Convergence tests

In this section, we numerically assess the behaviour of our scheme with respect to mesh refinement. We consider $\Omega = (0, 1)^2$ and solve Problem (25) choosing f such that

$$u(x, y) = x(1-x)y(1-y),$$

$$\boldsymbol{\sigma}(x, y) = \nabla u(x, y) = \begin{pmatrix} (1-2x)y(1-y) \\ x(1-x)(1-2y) \end{pmatrix}.$$

First, we consider the four families of meshes depicted in Figure 2. We assess the method behaviour by computing the following relative errors:

$$\text{err}_u = \frac{1}{\|u\|_0} \left(\sum_{E \in \mathcal{M}_h} \|u - u_h\|_{0,E}^2 \right)^{\frac{1}{2}},$$

$$\text{err}_{\text{div}} = \frac{1}{\|\text{div } \boldsymbol{\sigma}\|_0} \sum_{E \in \mathcal{M}_h} \left(\|\text{div } \boldsymbol{\sigma} - \text{div } \boldsymbol{\sigma}_h\|_{0,E}^2 \right)^{\frac{1}{2}},$$

$$\text{err}_{\boldsymbol{\sigma}} = \frac{1}{\|\boldsymbol{\sigma}\|_0} \left(\sum_{E \in \mathcal{M}_h} \left\| \boldsymbol{\sigma} - \hat{\Pi}_{k-1,E}^0 \boldsymbol{\sigma}_h \right\|_{0,E}^2 \right)^{\frac{1}{2}},$$

$$\text{err}_{\boldsymbol{\sigma} \cdot \mathbf{n}} = \frac{\left(\sum_{e \in \mathcal{E}_h} h_e \|\boldsymbol{\sigma} - \boldsymbol{\sigma}_h\|_{0,e} \right)^{\frac{1}{2}}}{\left(\sum_{e \in \mathcal{E}_h} h_e \|\boldsymbol{\sigma} \cdot \mathbf{n}^e\|_{0,e} \right)^{\frac{1}{2}}},$$

where \mathcal{E}_h denotes the set all edges of \mathcal{M}_h . We also solve the test problem with the standard VEM method [4]. We recall that for this latter method, the local discrete bilinear form $a_h(\cdot, \cdot)$ is given by

$$a_h^E(\boldsymbol{\sigma}_h, \boldsymbol{\tau}_h) = (\Pi_{0,E}^0 \boldsymbol{\sigma}_h, \Pi_{0,E}^0 \boldsymbol{\tau}_h)_E + s^E((I - \Pi_{0,E}^0) \boldsymbol{\sigma}_h, (I - \Pi_{0,E}^0) \boldsymbol{\tau}_h), \quad (65)$$

where $s^E(\cdot, \cdot)$ is the local stabilization term. In matrix form, the stabilization term we choose is given by

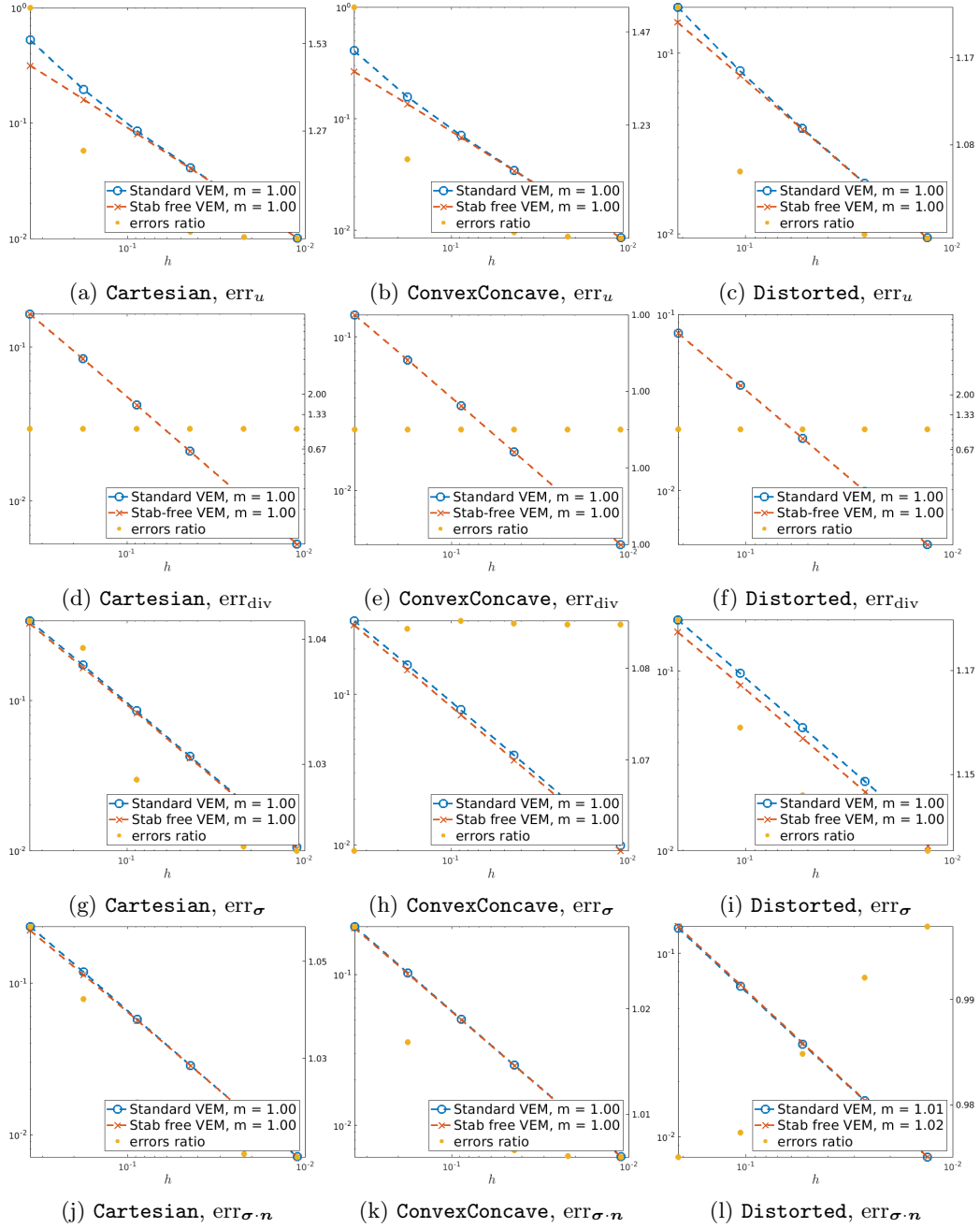


Figure 3: Convergence curves on quadrilateral meshes. The left vertical axis refers to the values of the errors (*dotted lines*). The right vertical axis refers to the ratio between the error made by the standard VEM method and the error of the proposed method (*orange dots*).

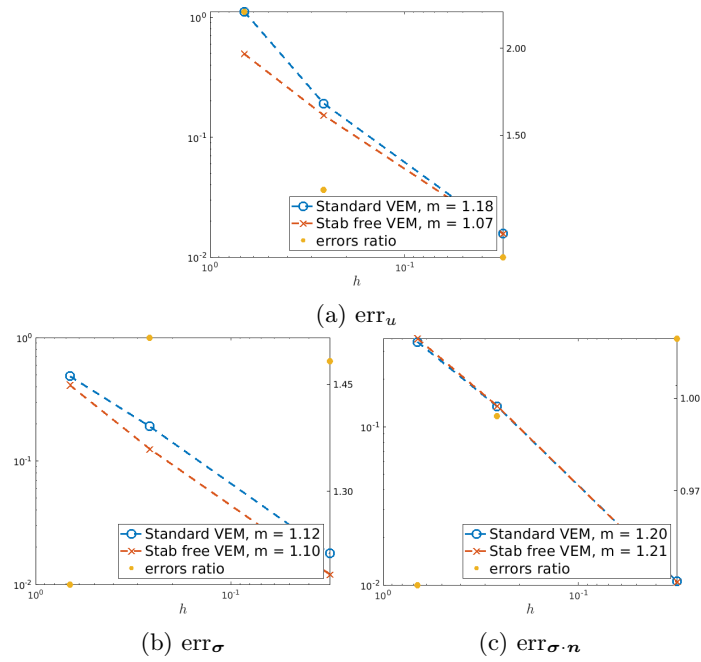


Figure 4: Convergence curves on **Random** mesh. The left vertical axis refers to the values of the errors (*dotted lines*). The right vertical axis refers to the ratio between the error made by the standard VEM method and the error of the proposed method (*orange dots*).

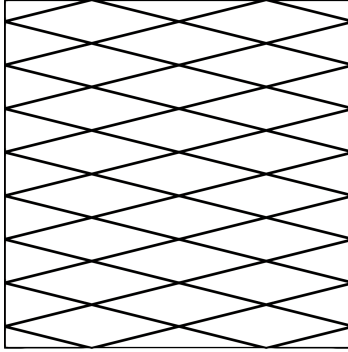


Figure 5: Rhomboidal mesh

$$\mathbf{S} = (\mathbf{I} - \mathbf{\Pi}^0)^T \mathbf{D} (\mathbf{I} - \mathbf{\Pi}^0), \quad (66)$$

where the matrix $\mathbf{\Pi}^0$ represents the projection onto the constant vector functions. Moreover, \mathbf{D} is a diagonal matrix defined as

$$\mathbf{D}_{ii} = \max \left(h_E |e_i|, (\mathbf{\Pi}_{0,E}^0 \varphi_i, \mathbf{\Pi}_{0,E}^0 \varphi_i)_E \right). \quad (67)$$

Above, the functions φ_i denote the elements of the Lagrangian basis corresponding to the local degrees of freedom (4). This choice is known as D-recipe stabilization, and it is inspired by the numerical assessment in [6, 26]. We also notice that in computing the error err_σ , for the standard VEM we use the projection onto constants.

In Figure 3, we consider the quadrilateral meshes of Figures 2a, 2b and 2c, respectively named **Cartesian**, **ConvexConcave** and **Distorted**. The computed errors obtained by the two methods are compared with respect to the maximum diameter of the mesh, denoted by h , and the asymptotical convergence rates are reported in the legend. The results show that the two methods behave equivalently on all meshes with respect to all the computed errors. We also remark that on all the meshes, both methods return exactly the same results for err_{div} . This is not surprising, since for all the meshes and both methods, from the second equation of (25) we get $\text{div } \sigma_h = -\mathbf{\Pi}_{0,E}^0 f$, while $\text{div } \sigma = -f$. Hence err_{div} is always the L^2 error when the load term f is approximated by piecewise constant functions. Accordingly, from now on we will not display that error quantity.

In Figure 2d we consider the family of meshes named **Random**, i.e. polygonal meshes obtained using *Polymesher* [33], whose elements are not only quadrilaterals. On each polygon, we construct the local bilinear form $a_h^E(\cdot, \cdot)$ (20) choosing k as in (19) (see Remark 1). As we can see in Figure 4, the proposed method is stable and exhibits the expected convergence rates.

6.2 Comparison with standard VEM on an anisotropic refinement test

In this section, we consider the problem presented in the previous section with a **Rhomboidal** mesh, as depicted in Figure 5. This mesh is refined applying an anisotropic rule. In particular, at each step the mesh is refined by a factor α in the x-direction and by a factor

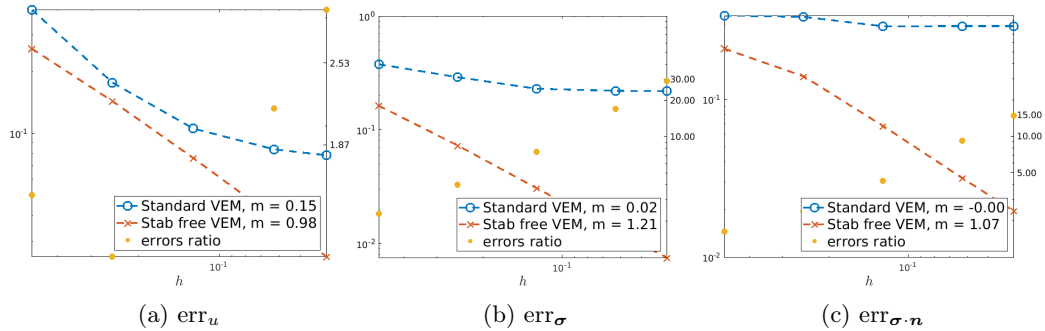


Figure 6: Convergence curves on Rhomboidal mesh. The left vertical axis refers to the values of the errors (*dotted lines*). The right vertical axis refers to the ratio between the error made by the standard VEM method and the error of the proposed method (*orange dots*).

α^2 in the y-direction. In Figure 6, we present the convergence plots. We observe that the standard VEM method is not properly converging, while the proposed scheme exhibit the expected convergence behaviour.

7 Conclusions

We have presented a self-stabilized Virtual Element Method for the Poisson problem in mixed form. One of the main features of our approach is the employment of a projection operator over the gradients of harmonic polynomials of suitable degree. This choice alleviates the computational costs arising from the numerical quadrature. Despite the scheme is designed for arbitrary polygons, the theoretical analysis has been developed only for quadrilateral meshes. The method convergence and stability have been computationally confirmed. Moreover, the numerical results show that our scheme is a valid alternative to the standard lowest-order mixed VEM.

A possible future development of the present study is the extension of the analysis to general polygonal meshes.

Acknowledgements

The authors kindly acknowledge partial financial support by INdAM-GNCS projects 2022 CUP_E55F2200027001. C.L. and M.V. kindly acknowledge partial financial support by PRIN 2017 (No. 201744KLJL) and PRIN 2020 (No. 20204LN5N5), funded by the Italian Ministry of Universities and Research (MUR). A.B and F.M. kindly acknowledge financial support provided by PNRR M4C2 project of CN0000013 National Centre for HPC, Big Data and Quantum Computing (HPC) CUP:E13C22000990001. A.B. kindly acknowledges partial financial support provided by INdAM-GNCS Projects 2023, MIUR project “Dipartimenti di Eccellenza” Programme (2018–2022) CUP:E11G18000350001 and by the PRIN 2020 project (No. 20204LN5N5_003).

References

- [1] E. Artioli, S. de Miranda, C. Lovadina, and L. Patruno. A stress/displacement virtual element method for plane elasticity problems. *Computer Methods in Applied Mechanics and Engineering*, 325:155–174, 2017.
- [2] L. Beirão da Veiga, F. Brezzi, A. Cangiani, G. Manzini, L. D. Marini, and A. Russo. Basic principles of virtual element methods. *Mathematical Models and Methods in Applied Sciences*, 23(01):199–214, 2013.
- [3] L. Beirão da Veiga, F. Brezzi, L. D. Marini, and A. Russo. $H(\text{div})$ and $H(\text{curl})$ -conforming virtual element methods. *Numerische Mathematik*, 133(2):303–332, 2016.
- [4] L. Beirão da Veiga, F. Brezzi, L. D. Marini, and A. Russo. Mixed virtual element methods for general second order elliptic problems on polygonal meshes. *ESAIM: Mathematical Modelling and Numerical Analysis*, 50(3):727–747, 2016.
- [5] L. Beirão da Veiga, C. Canuto, R. H. Nochetto, G. Vacca, and M. Verani. Adaptive VEM: Stabilization-free a posteriori error analysis and contraction property. arXiv:2111.07656, 2021.
- [6] L. Beirão da Veiga, F. Dassi, and A. Russo. High-order virtual element method on polyhedral meshes. *Computers and Mathematics with Applications*, 74, 2017.
- [7] L. Beirão da Veiga, C. Lovadina, and D. Mora. A virtual element method for elastic and inelastic problems on polytope meshes. *Computer Methods in Applied Mechanics and Engineering*, 295:327–346, 2015.
- [8] M. F. Benedetto, S. Berrone, and A. Borio. The Virtual Element Method for underground flow simulations in fractured media. In *Advances in Discretization Methods*, volume 12 of *SEMA SIMAI Springer Series*, pages 167–186. Springer International Publishing, Switzerland, 2016.
- [9] M. F. Benedetto, S. Berrone, A. Borio, S. Pieraccini, and S. Scialò. A hybrid mortar virtual element method for discrete fracture network simulations. *Journal of Computational Physics*, 306:148–166, 2016.
- [10] M.F. Benedetto, A. Borio, F. Kyburg, J. Mollica, and S. Scialò. An arbitrary order mixed virtual element formulation for coupled multi-dimensional flow problems. *Computer Methods in Applied Mechanics and Engineering*, 391:114204, 2022.
- [11] S. Berrone and A. Borio. A residual a posteriori error estimate for the virtual element method. *Mathematical Models and Methods in Applied Sciences*, 27(08):1423–1458, 2017.
- [12] S. Berrone, A. Borio, and F. Marcon. Lowest order stabilization free Virtual Element Method for the Poisson equation. arXiv:2103.16896, 2021.
- [13] S. Berrone, A. Borio, and F. Marcon. Comparison of standard and stabilization free Virtual Elements on anisotropic elliptic problems. *Applied Mathematics Letters*, 129:107971, 2022.

- [14] S. Berrone and M. Busetto. A virtual element method for the two-phase flow of immiscible fluids in porous media. *Computational Geosciences*, 26:195–216, 2022.
- [15] S. Berrone, M. Busetto, and F. Vicini. Virtual element simulation of two-phase flow of immiscible fluids in discrete fracture networks. *Journal of Computational Physics*, 473:111735, 2023.
- [16] Stefano Berrone, Andrea Borio, Alessandro D’Auria, Stefano Scialò, and Fabio Vicini. A robust vem-based approach for flow simulations in poro-fractured media. *Mathematical Models and Methods in Applied Sciences*, 31(14):2855–2885, 2021.
- [17] Stefano Berrone, Andrea Borio, Francesca Marcon, and Gioana Teora. A first-order stabilization-free virtual element method. *Applied Mathematics Letters*, 142:108641, 2023.
- [18] D. Boffi, F. Brezzi, and M. Fortin. *Mixed Finite Element Methods and Applications*. Springer Berlin Heidelberg, 2013.
- [19] Andrea Borio, François P. Hamon, Nicola Castelletto, Joshua A. White, and Randolph R. Settgast. Hybrid mimetic finite-difference and virtual element formulation for coupled poromechanics. *Computer Methods in Applied Mechanics and Engineering*, 383:113917, 2021.
- [20] J. H. Bramble and S. R. Hilbert. Estimation of linear functionals on Sobolev spaces with application to fourier transforms and spline interpolation. *SIAM journal on numerical analysis*, 7(1):112–124, 1970.
- [21] S. C. Brenner and L. R. Scott. *The mathematical theory of finite element methods*, volume 15 of *Texts in Applied Mathematics*. Springer, New York, third edition, 2008.
- [22] F. Brezzi, Richard S. Falk, and L. D. Marini. Basic principles of mixed virtual element methods. *ESAIM: Mathematical Modelling and Numerical Analysis*, 48(4):1227–1240, 2014.
- [23] A. Cangiani, E. H. Georgoulis, T. Pryer, and O. J. Sutton. A posteriori error estimates for the virtual element method. *Numerische Mathematik*, 137(4):857–893, Dec 2017.
- [24] H. S. M Coxeter and Samuel L Greitzer. *Geometry revisited*, volume 19 of *Anneli Lax New Mathematical Library*. Random House, New York, 1 edition, 1967.
- [25] F. Dassi, C. Lovadina, and M. Visinoni. A three-dimensional Hellinger–Reissner virtual element method for linear elasticity problems. *Computer Methods in Applied Mechanics and Engineering*, 364:112910, 2020.
- [26] F. Dassi and L. Mascotto. Exploring high-order three dimensional virtual elements: Bases and stabilizations. *Computers and Mathematics with Applications*, 75, 2018.
- [27] F. Dassi and G. Vacca. Bricks for the mixed high-order virtual element method: Projectors and differential operators. *Applied Numerical Mathematics*, 155:140–159, 2020.
- [28] Franco Dassi, Carlo Lovadina, and Michele Visinoni. Hybridization of the virtual element method for linear elasticity problems. *Mathematical Models and Methods in Applied Sciences*, 31(14):2979–3008, 2021.

- [29] T. Dupont and L. R. Scott. Polynomial approximation of functions in sobolev spaces. *Mathematics of computation*, 34(150):441–463, 1980.
- [30] A.M. D’Altri, S. de Miranda, L. Patruno, and E. Sacco. An enhanced vem formulation for plane elasticity. *Computer Methods in Applied Mechanics and Engineering*, 376:113663, 2021.
- [31] A. Lamperti, M. Cremonesi, U. Perego, C. Lovadina, and A. Russo. A Hu-Washizu variational approach to self-stabilized Virtual Elements: 2D linear elastostatics. *Computational Mechanics*, 71:935–955, 2023.
- [32] A. Sommariva and M. Vianello. Product Gauss cubature over polygons based on Green’s integration formula. *BIT Numerical Mathematics*, 47(2):441 – 453, 2007.
- [33] C. Talischi, G. H. Paulino, A. Pereira, and I. F. M. Menezes. Polymesher: A general-purpose mesh generator for polygonal elements written in matlab. *Struct. Multidiscipl. Optim.*, 45(3):309–328, 2012.